An empirical torque relation for supercritical flow between rotating cylinders

By R. J. DONNELLY AND N. J. SIMON
Institute for the Study of Metals and Department of Physics,
The University of Chicago, Chicago, Illinois

(Received 16 July 1959)

An empirical relationship for the torque transmitted by fluid friction to an outer cylinder as a function of the angular velocity of the inner cylinder has been obtained by analysis of experimental data published by Wendt, Taylor and Donnelly. With one exception it is found that the torque G has the functional form

$$G = a\Omega_1^{-1} + b\Omega_1^{1\cdot36},$$

where Ω_1 is the angular velocity of the inner cylinder and a and b are constants determined from the data. The formula applies to a range of values of Ω_1 above the onset of instability extending to about 10 times the critical angular velocity. The experiments also show that the finite amplitude analysis recently advanced by Stuart gives the correct variation of torque over a short range above the critical speed. At speeds well beyond critical it is found that G varies approximately as $\Omega_1^{1\cdot5}$, and that the variation of torque with gap width can be expressed as a simple power law with exponent about 0·31. In an appendix Dr G. K. Batchelor shows that these latter relations are consistent with the supposition that the flow is steady and consists of inviscid cores surrounded by boundary layers.

1. Introduction

The study of the flow of a viscous liquid between rotating cylinders has been a very important and fruitful area of investigation in fluid mechanics. Linear stability theory has had its greatest success in the prediction of the onset of instability in this geometry. It is natural, therefore, to try to obtain a description of the unstable flow as a means of studying the transition to turbulence.

Experimentally, two techniques commonly used are the observation of dye traces in the fluid and the measurement of the torque transmitted to one cylinder as a function of the angular velocity of the other. The first of these is well suited to the observation of flow patterns up to the onset of instability, but is of less value as the motions of the fluid become more rapid and complicated. Suspensions of fine particles such as aluminium pigment (cf. Schultz-Grunow & Hein 1956) overcome some of the difficulties. The torque method, while applied so far only to the case where one cylinder is at rest, has the advantage that the results can be compared quantitatively with theory.

Recently Stuart (1958) has advanced an analysis which enabled him to calculate the relationship between the torque on the outer cylinder and the angular

velocity of the inner cylinder, if the two cylinders have nearly equal radii. He has compared his results with measurements by Taylor (1936). Since increasing attention is being given to finite amplitude problems, we have analyzed all the available published torque measurements of this kind in order to provide a basis for comparison with theory. The results may also provide some guide as to the selection of suitable assumptions for calculations.

2. Theoretical relations

When the flow is laminar the torque G transmitted to the outer cylinder as a function of the rate of rotation of the inner cylinder Ω_1 is

$$G = \frac{4\pi\eta R_1^2 R_2^2 h\Omega_1}{R_2^2 - R_1^2}. \tag{1}$$

Here η is the viscosity of the fluid, R_1 and R_2 are the radii of the cylinders ($R_2 > R_1$) and h is the length of the outer cylinder. Equation (1) is exact and forms the basis for the absolute determination of viscosity. At speeds near the onset of instability, small deviations from (1) possibly due to the finite length of the cylinders or incorrect alignment may be observed (Donnelly 1958).

The validity of (1) is limited by the onset of instability in the laminar flow with formation of vortices as described first by Taylor (1923). The value of Ω_1 at which instability begins, which we shall call Ω_c, is calculated from the critical Taylor number. For the case of a 'narrow gap' the Taylor number (Chandrasekhar 1954) is defined as

$$T = \frac{4R_1^2 d^4}{R_2^2 - R_1^2}\left(\frac{\Omega_1}{\nu}\right)^2 \quad (d \ll r_0), \tag{2}$$

where

$$d = R_2 - R_1, \tag{3}$$

$$r_0 = \tfrac{1}{2}(R_1 + R_2), \tag{4}$$

$\nu\,(= \eta/\rho)$ is the kinematic viscosity of the liquid and ρ is the density. The critical Taylor number here is

$$T_c = 3{\cdot}390 \times 10^3. \tag{5}$$

It should be emphasized that in all these formulae we assume that the outer cylinder is at rest. Another approximation, used by Stuart in the calculations quoted below, is

$$T = R_1 d^3(\Omega_1/\nu)^2, \tag{6}$$

$$T_c = 1{\cdot}708 \times 10^3. \tag{7}$$

In the limit $d \to 0$ the expressions (2) and (6) are identical (except for a factor 2) and the values of Ω_c calculated from the critical numbers are very close.

When the gap between cylinders is finite a different analysis of the stability problem is required (Chandrasekhar 1958). Numerical calculations have been given only for the case of $R_1/R_2 = \frac{1}{2}$. Here the appropriate Taylor number is

$$T = \tfrac{64}{9}R_1^4\left(\frac{\Omega_1}{\nu}\right)^2 \quad (R_1/R_2 = \tfrac{1}{2}) \tag{8}$$

and

$$T_c = 3{\cdot}310 \times 10^4. \tag{9}$$

A calculation of the torque for values of Ω beyond Ω_c has been made by Stuart (1958) on the basis of a finite amplitude theory. His result may be written

$$G = 2\pi R_1^2 h\eta \left|\frac{\partial \bar{v}}{\partial r}\right|_{r=R_1}, \tag{10}$$

where

$$\left|\frac{\partial \bar{v}}{\partial r}\right|_{r=R_1} = \frac{\Omega_1 r_0}{d}\left[1+\mathscr{D}\left(1-\frac{T_c}{T}\right)\right] \quad (d \ll r_0,\ T-T_c \to 0). \tag{11}$$

T and T_c are given in (6) and (7) and $\mathscr{D}$ is a constant which follows from the formulae given on p. 18 of Stuart's paper. In the notation of that paper

$$\mathscr{D} = \left\{\int_{-\frac{1}{2}}^{\frac{1}{2}} Z^2 d\zeta \left(\int_{-\frac{1}{2}}^{\frac{1}{2}} Z\, d\zeta\right)^{-2} - 1\right\}^{-1} = 1{\cdot}4472. \tag{12}$$

For purposes of comparison with experiment we may rewrite (10) and (11) in the form

$$G = a\Omega_1^{-1} + b\Omega_1 \quad (\Omega_1 > \Omega_c), \tag{13}$$

where

$$a = -(2\pi R_1 h\eta r_0 \nu^2)(\mathscr{D}T_c)/d^4 \tag{14}$$

and

$$b = (2\pi R_1^2 h\eta r_0)(1+\mathscr{D})/d. \tag{15}$$

As suggested by (11), Stuart's analysis is valid for the 'narrow gap' geometry and is not expected to hold for values of T much above T_c.

From dimensional considerations one can see that the general expression for the torque must be of the form

$$G/\rho h\Omega_1^2 R_1^4 \propto f(R, d/R_1) \tag{16}$$

provided only the inner cylinder rotates. Here the Reynolds number is defined as

$$R = \Omega_1 R_1 d/\nu. \tag{17}$$

Dr G. K. Batchelor shows in an appendix to this paper that a prediction for the form of the function f can be made for speeds well above critical using the 'inviscid-core-and-boundary-layer' model of the flow (Batchelor 1956). The result of such an argument leads to

$$G/\rho h\Omega_1^2 R_1^4 \propto R^{-\frac{1}{2}}(d/R_1)^{\frac{1}{4}}. \tag{18}$$

In §§3–5 we shall discuss the variation of torque with angular velocity. In §6 we shall consider the evidence for the variation of torque with gap width at high speeds.

3. Reduction of the data

Torque measurements of the type we are discussing have been reported by Wendt (1933), Taylor (1936) and Donnelly (1958). Since the first two authors did not publish tables of measurements, we have photographed and enlarged the graphs and taken the data from them with calipers. Due to mechanical limitations of the apparatus several fluids must be used to determine a complete (G, Ω_1)-curve. Dynamical similarity requires that for any given pair of radii $G/\rho\Omega_1^2$ must be a function of Ω_1/ν. It is customary to calculate these quantities (or equivalent dimensionless parameters) for each fluid and combine them on a single curve.

On such a graph the laminar flow line starts at the upper left and extends to the lower right. The data leave this line at the critical speed (see figure 1).

For theoretical purposes the different fluids are of little interest, so that the empirical relations below have been quoted for the fluid of greatest viscosity. From the discussion above we see that if two fluids are measured at the same value of Ω_1/ν in the same apparatus, the same value of $G/\rho\Omega_1^2$ is obtained. We can then convert the torque data from liquid 2 to the equivalent for liquid 1 by the relation

$$G_1 = \left(\frac{\rho_1 \nu_1^2}{\rho_2 \nu_2^2}\right) G_2. \tag{19}$$

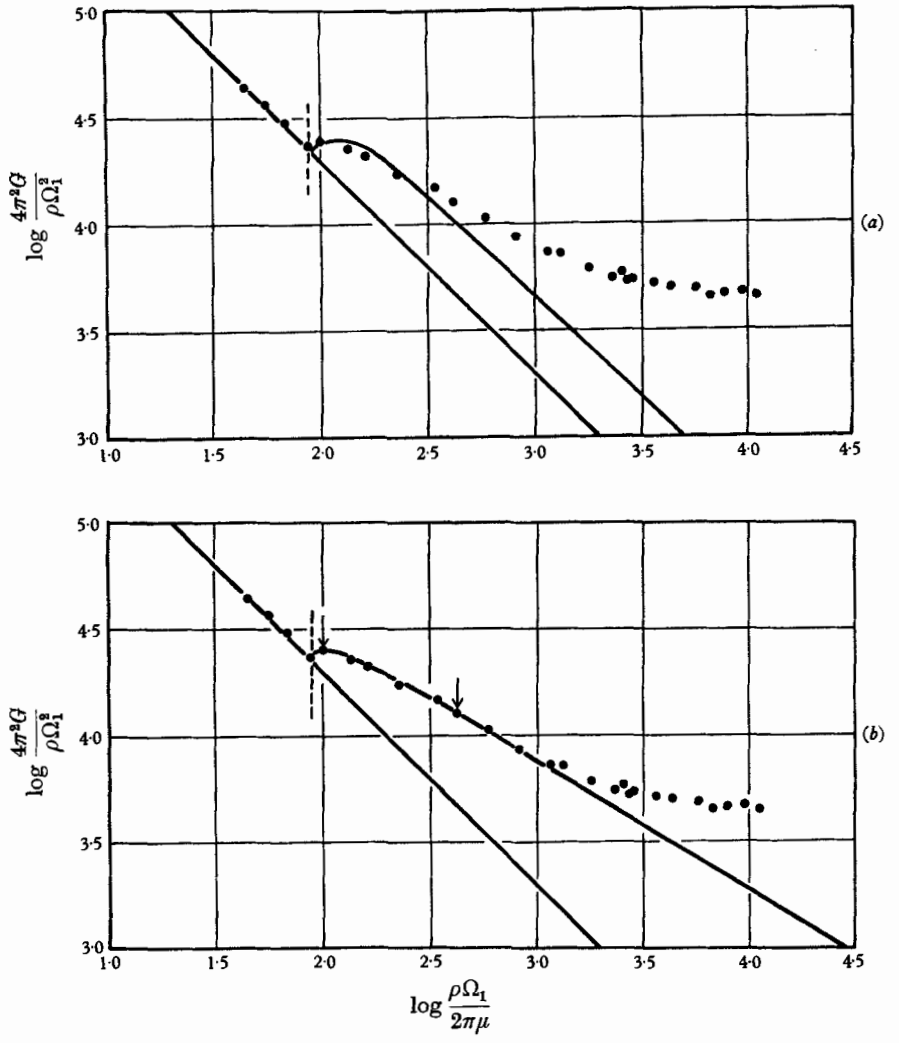

FIGURE 1. (*a*) After Taylor (1936, Fig. 2). $R_2 = 4{\cdot}05$ cm, $R_1 = 3{\cdot}94$ cm, $\nu = 0{\cdot}131$, $\rho = 1{\cdot}171$. The dashed line corresponds to the calculated value of Ω_c. The solid line corresponds to $G = -3{\cdot}71 \times 10^8 \Omega_1^{-1} + 1{\cdot}12 \times 10^5 \Omega_1$, calculated from Stuart's formula. (*b*) Data as in (*a*). The solid line corresponds to $G = -1{\cdot}21 \times 10^8 \Omega_1^{-1} + 1{\cdot}59 \times 10^4 \Omega_1^{1{\cdot}36}$, fitted empirically.

The notation and constants of the experiments are listed below.

(*a*) *Measurements of Taylor*

G = measured torque in g cm^2 sec^{-2};
ρ = density of fluid in g/cm^3 = 1·171 g/cm^3;
ν = 0·131 cm^2/sec;
h = 84·4 cm.

Taylor made measurements with R_2 = 4·05 cm and inner cylinders of the following sizes:

R_1 = 3·94 (figure 1), 3·89 (figure 2), 3·83, 3·74, 3·68, 3·59, 3·45 and 3·20 cm.

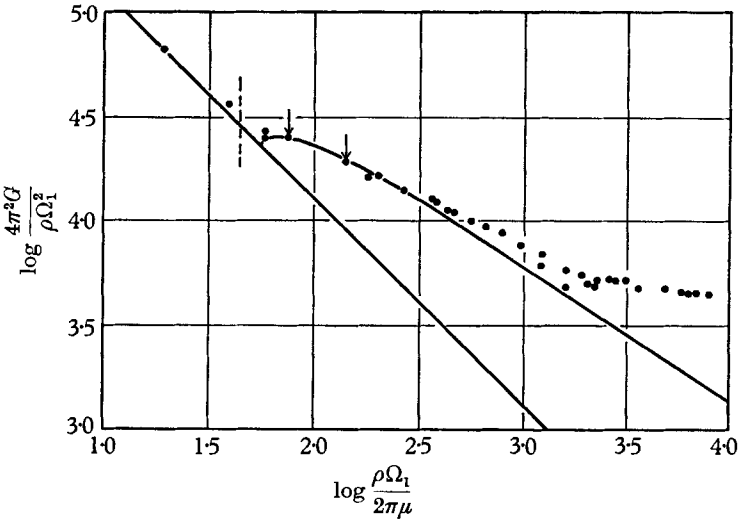

FIGURE 2. After Taylor (1936, Fig. 3). R_1 = 3·89 cm, R_2 = 4·05 cm, ν = 0·131, ρ = 1·171. The curve corresponds to $G = -4{\cdot}41 \times 10^7\, \Omega_1^{-1} + 1{\cdot}28 \times 10^4\, \Omega_1^{1{\cdot}36}$.

(*b*) *Measurements of Wendt*

R_2 = 14·70 cm;
R_1 = 13·75 cm (figure 3), 12·50 cm (figure 4), 10·00 cm (figure 5);
$\lambda = \tau_i/\frac{1}{2}\rho\Omega_1^2 R_1^2 = G/\pi h\rho\Omega_1^2 R_1^4$, where τ_i is the stress on the inner cylinder.

As Wendt did not list the viscosity of his liquids, which were pure water and glycerine–water solutions, we have reduced his data by defining

$$\mathrm{T} = \tau_i/\tfrac{1}{2}\rho\nu^2, \quad U = \Omega_1 R_1/\nu, \tag{20}$$

so that $\lambda = \mathrm{T}/U^2$. Thus T is proportional to the torque and U is proportional to Ω_1 (for constant ν, R_1 and R_2).

(*c*) *Measurements of Donnelly*

G = torque in dyne cm;
h = 4·998 ± 0·0003 cm;
R_2 = 2·00023 ± 0·0001 cm;
R_1 = 1·89936 ± 0·0001 cm in figures 6 and 7,
= 0·99963 ± 0·0001 cm in figures 8 and 9;

$\nu = 5{\cdot}796 \times 10^{-3}$ in figures 6 and 7,
$= 1{\cdot}226 \times 10^{-1}$ in figures 8 and 9;
$\rho = 1{\cdot}585\,\mathrm{g/cm^3}$ in figures 6 and 7,
$= 0{\cdot}8404\,\mathrm{g/cm^3}$ in figures 8 and 9.

The original data are presented in tables 1 and 2. G is given as a function of the Reynolds number R and (19) has been used to convert all the data to the equivalent torque for the liquid of greatest kinematic viscosity.

G (dyne cm)	R	G (dyne cm)	R	G (dyne cm)	R
13·0	20·8	108	174	292	297
14·2	22·9	113	181	328	318
16·3	26·3	116	183	382	346
18·5	30·0	120	185	547	431
21·5	34·7	124	188	597	452
25·9	41·6	127	189	633	470
32·2	51·9	130	190	641	482
43·0	69·2	134	192	755	549
64·5	104	140	195	786	568
72·1	116	147	200	924	634
76·2	122	151	204	1090	710
80·8	129	160	210	1330	825
82·2	138	173	219	1580	920
92·9	149	183	231	1858	1026
100	160	220	254	2209	1165
104	167	256	276		

TABLE 1. Torque measurements as a function of Reynolds number ($R_1 = 1{\cdot}9$ cm, $R_2 = 2{\cdot}0$ cm, $h = 5{\cdot}0$ cm, $\nu = 5{\cdot}796 \times 10^{-3}$ cm²/sec, $\rho = 1{\cdot}585$ g/cm³, $R = \Omega_1 R_1 d/\nu$)

G (dyne cm)	R	G (dyne cm)	R	G (dyne cm)	R
10·8	10·2	70·4	65·5	180	121
12·1	11·4	71·4	66·6	198	127
13·6	12·8	72·5	67·4	240	149
15·5	14·6	72·9	67·8	283	167
18·1	17·1	73·6	68·2	345	192
21·8	20·5	74·9	69·1	808	360
27·2	25·6	76·7	70·2	1430	541
36·2	34·1	82·0	73·0	1710	619
45·4	42·7	86·5	75·3	2150	722
54·5	51·1	93·4	78·8	2680	867
57·4	53·9	106	85·1	2830	901
60·6	56·9	116	92·7	3690	1050
64·0	60·1	126	94·8	5450	1440
68·3	63·9	146	107	8990	2040

TABLE 2. Torque measurements as a function of Reynolds number ($R_1 = 1{\cdot}0$ cm, $R_2 = 2{\cdot}0$ cm, $h = 5{\cdot}0$ cm, $\nu = 0{\cdot}1226$ cm²/sec, $\rho = 0{\cdot}8404$ g/cm³, $R = \Omega_1 R_1 d/\nu = \Omega_1 R_1^2/\nu$)

4. The variation of torque with angular velocity

From the discussion in §2 we see that the torque can be computed by (1) up to a known Ω_c. Above Ω_c, Stuart's equation (13) can be used. A comparison of (13) with Taylor's data is shown in figure 1*a*. From (14) and (15) and the dimensions in §3 we find

$$a = -3{\cdot}71 \times 10^8, \quad b = 1{\cdot}12 \times 10^5.$$

The fit as $T - T_c \to 0$ is quite accurate, the dominant term being that in Ω_1^{-1}. This is the expected range of validity of the theory. At higher speeds (13) is dominated by the linear term and the curve becomes parallel to the laminar flow line. A comparison with data of Donnelly may be seen in figure 7.

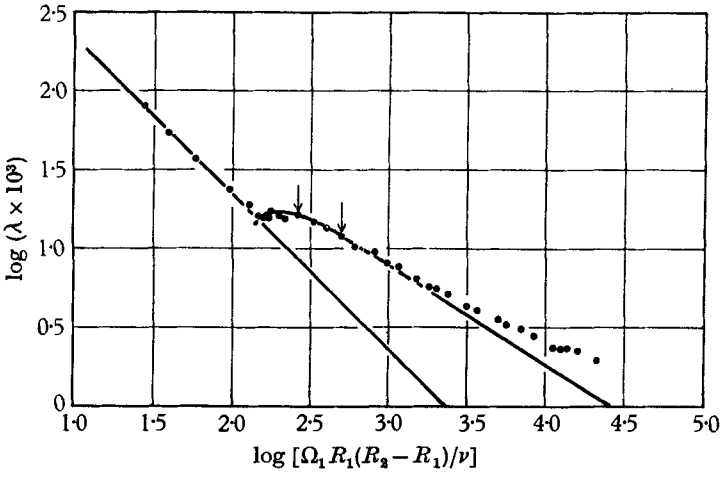

FIGURE 3. After Wendt (1933, Abb. 13). $R_1 = 13{\cdot}75$ cm, $R_2 = 14{\cdot}70$ cm. The curve corresponds to $T = -4{\cdot}46 \times 10^4 U^{-1} + 0{\cdot}650 U^{1{\cdot}36}$.

An examination of figure 1*a* shows that the data for $\Omega \gg \Omega_c$ follow a straight line, but with a higher power of Ω_1. Figure 1*b* shows the result of assuming that the torque relation has the form

$$G = a\Omega_1^{-1} + b\Omega_1^n \quad (\Omega > \Omega_c), \tag{21}$$

with $n = 1{\cdot}36$. The constants a and b have been determined by the points marked with arrows. It can be seen that (21) fits the data within experimental error in the range $1{\cdot}9 < \log(\rho\Omega_1/2\pi\mu) < 3{\cdot}1$, or over a factor of 16 above Ω_c. Since $T \propto \Omega_1^2$, this corresponds to agreement over a range of about $256T_c$. The value of n in (21) appears to be the same for all the experiments, as will be shown below. Therefore we will use the form

$$G = a\Omega_1^{-1} + b\Omega_1^{1{\cdot}36} \quad (\Omega_1 > \Omega_c) \tag{22}$$

for all the data.

A second measurement by Taylor is shown in figure 2. The solid line is calculated from (22) and the marked points. It holds within experimental error over the range $1{\cdot}75 < \log\rho\Omega_1/2\pi\mu < 2{\cdot}5$, or up to values of Ω near $6\Omega_c$. The deviation at $\log(\rho\Omega_1/2\pi\mu) = 3{\cdot}0$ amounts to 20 %.

The data of Wendt are shown in figures 3–5. As explained in §3 we have used T and U instead of G and Ω_1 in (22). The solid line represents the data in figure 3 over the range $2{\cdot}2 < \log R < 3{\cdot}3$, or up to values of Ω near $13\Omega_c$. The deviation at $\log R = 4{\cdot}0$ is 35 % from the empirical curve.

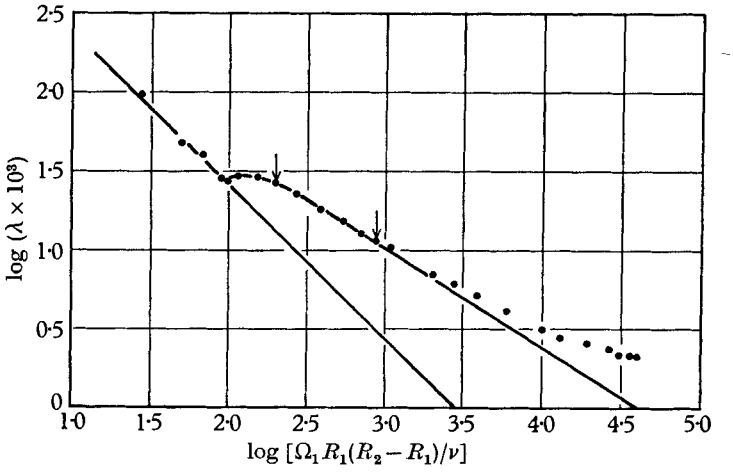

FIGURE 4. After Wendt (1933, Abb. 13). $R_1 = 12{\cdot}50$ cm, $R_2 = 14{\cdot}70$ cm. The curve corresponds to $\mathrm{T} = -1{\cdot}60 \times 10^3 U^{-1} + 0{\cdot}506 U^{1{\cdot}36}$.

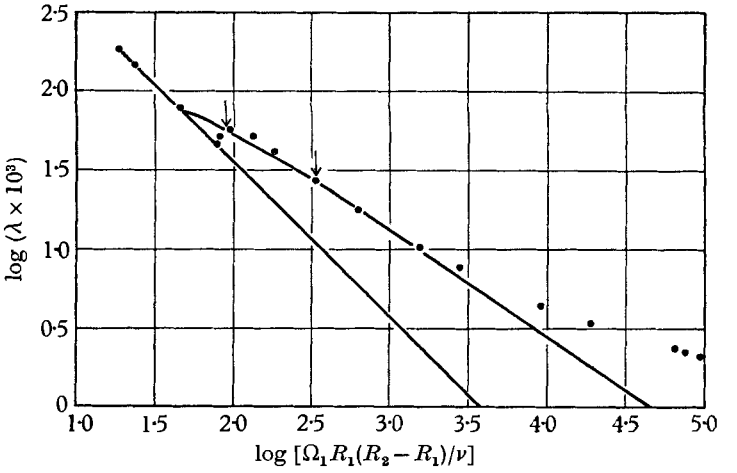

FIGURE 5. After Wendt (1933, Abb. 13). $R_1 = 10{\cdot}00$ cm, $R_2 = 14{\cdot}70$ cm. The form given by (22) will not represent this data accurately. The curve shown is

$$\mathrm{T} = -15 U^{-1} + 0{\cdot}387 U^{1{\cdot}36}.$$

In figure 4 the empirical curve fits over even a wider range: $2{\cdot}0 < \log R < 3{\cdot}3$, or up to $\Omega = 20\Omega_c$. The deviation at $\log R = 4{\cdot}0$ is 35% from the solid line.

The relation (22) is less successful for Wendt's widest gap arrangement, shown in figure 5. The curve may be made to fit either the beginning portion or the straight line portion of the measurements (as shown), but not both. There is a possibility that (22) breaks down for wide gap geometries. However, a comparison

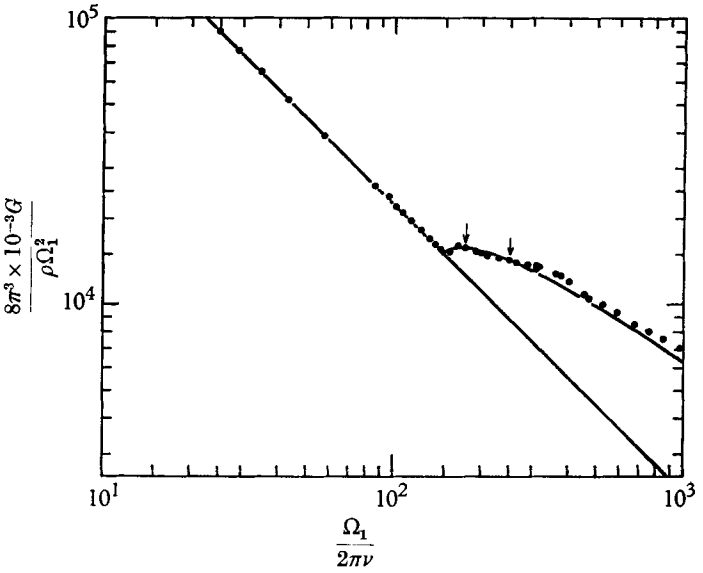

FIGURE 6. After Donnelly (1958, Fig. 5). $R_1 = 1{\cdot}9$ cm, $R_2 = 2{\cdot}0$ cm, $\nu = 5{\cdot}796 \times 10^{-3}$, $\rho = 1{\cdot}585$. The curve corresponds to $G = -254\,\Omega_1^{-1} + 16{\cdot}0\,\Omega_1^{1.36}$.

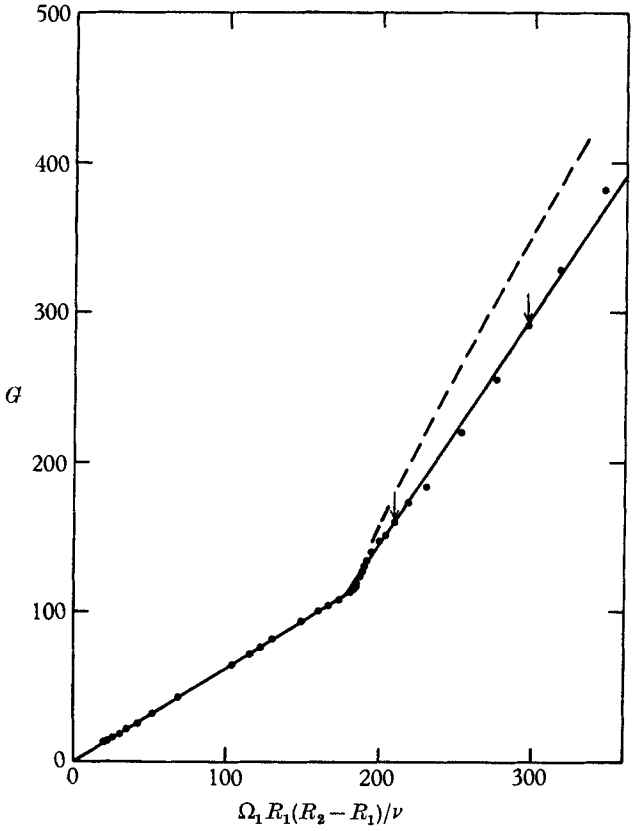

FIGURE 7. Plot of torque as a function of Reynolds number of the data in figure 6 and table 1. The dashed line corresponds to $G = -857\,\Omega_1^{-1} + 49{\cdot}2\,\Omega_1$, calculated from Stuart's formula.

of figures 6 and 8 which represent narrow and wide gap measurements shows that both follow (22).

The measurements of Donnelly are shown in figure 6 for the case $R_1 = 1{\cdot}9$ cm, $R_2 = 2{\cdot}0$ cm. The solid line is seen to fit the data fairly closely over the whole range, or to $7\Omega_c$. The detailed nature of the observations seem to indicate reproducible features which are not followed by the curve. In order to illustrate more clearly the nature of these deviations a linear plot of the original data near $\Omega = \Omega_c$, taken from table 1, is shown in figure 7. One can seen that the deviations from the curve are less than 3% in this range. It should be noticed that Wendt's data in figure 3 also show such deviations near Ω_c in a similar case: $d = 0{\cdot}0667\, r_0$ for figure 3 and $d = 0{\cdot}0513\, r_0$ for figures 6 and 7.

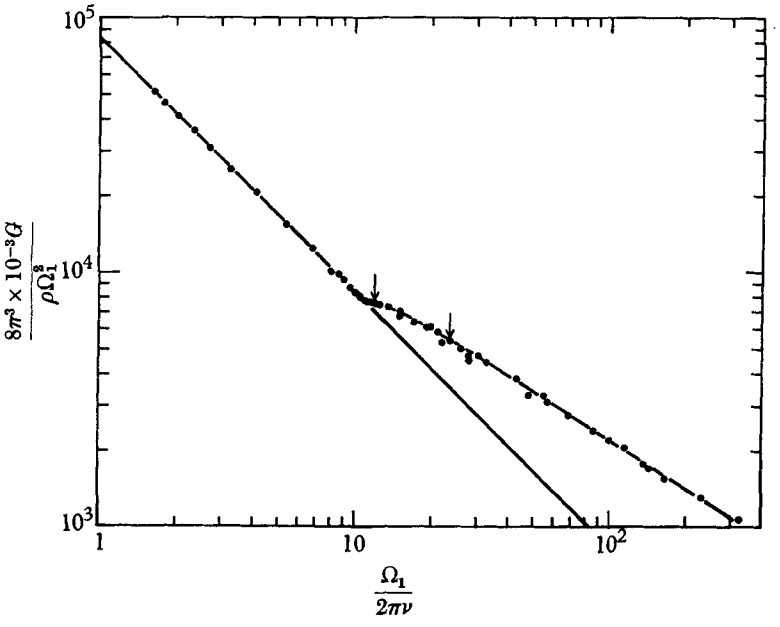

FIGURE 8. After Donnelly (1958, Fig. 8). $R_1 = 1{\cdot}0$ cm, $R_2 = 2{\cdot}0$ cm, $\nu = 0{\cdot}1226$, $\rho = 0{\cdot}8404$. The curve shown is $G = -104\ \Omega_1^{-1} + 4{\cdot}70\ \Omega_1^{1{\cdot}364}$.

We have calculated Stuart's torque relation (13) for this case and find

$$a = -857, \quad b = 49{\cdot}2.$$

This is plotted as a dashed line in figure 7. The calculated curve agrees with experiment very closely near the critical value (which is its intended range). The experimental critical point agrees with that calculated from (2) and (5) or (6) and (7) within 1%. At $\Omega_1 R_1 d/\nu = 300$ the calculated torque is about 20% too high.

Figure 8 shows measurements for the case $R_1 = 1{\cdot}0$ cm, $R_2 = 2{\cdot}0$ cm. Here (22) appears to represent the data within experimental error over the entire range of measurements, i.e. to 30 Ω_c or 900 T_c. The experimental data are given in table 2, and the fit near Ω_c is displayed on a linear scale in figure 9. The experimental value of Ω_c agrees with the value calculated from (8) and (9) to within $\frac{1}{2}$%.

We have made some studies to determine the experimental limits of the exponent n in (21). Wendt has suggested $n = 1{\cdot}5$ in his paper (cf. §6). We have tried several curves with $n = 1{\cdot}5$ and conclude that this represents the upper limit of the exponent for a close representation of the data in the range of interest here. The value $n = 1{\cdot}36$, which was determined from figure 8, appears to be the best compromise for all the measurements illustrated here, and at the same time

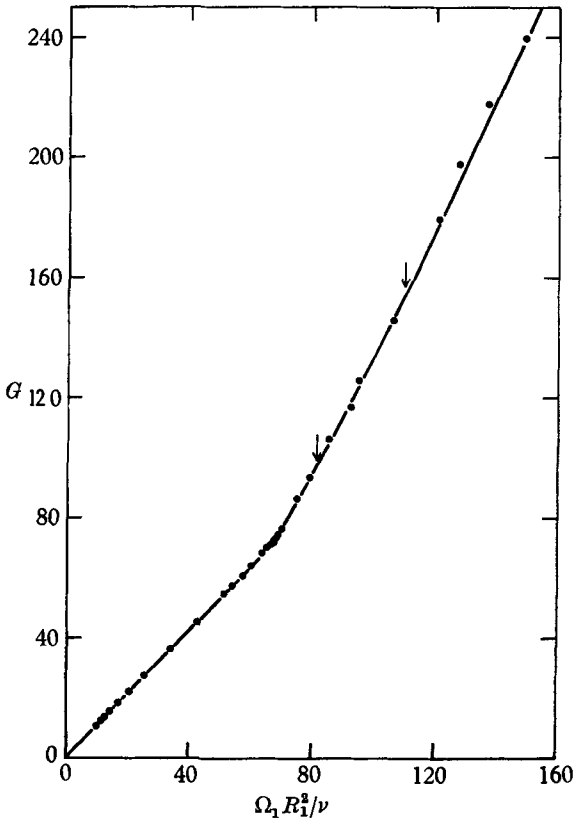

FIGURE 9. Plot of torque as a function of Reynolds number of the data in figure 8 and table 2.

Author	Figure	Range of approximation		Deviation from data	
Taylor	1*b*	$16 \times \Omega_c$	$256 \times T_c$	40 % at	$40 \times \Omega_c$
	2	6	36	20	18
Wendt	3	13	169	35	64
	4	20	400	35	100
	5	Fails	—	—	—
Donnelly	6	7*	49	8	7
	8	30	900	0	30

* Total range measured. Data deviates on both sides of curve: see §4.

TABLE 3. Range of validity of the empirical relation (22)

to be very near the lower limit of n. We may say that the experiments give $\frac{4}{3} < n < \frac{3}{2}$ with the smaller value somewhat closer to the best compromise. The range of validity is summarized in table 3.

5. Discussion

The experiments shown in figures 1*a* and 7 confirm the validity of the torque relation (13) given by Stuart over its intended range: $T \to T_c$ from above and $d \ll r_0$. The mechanism proposed by Stuart accounts for the general variation of torque even though detailed numerical agreement is limited to a short range above the critical Taylor number. The experimental evidence suggests that a relation of the form given in (22), which is a modification of Stuart's calculated equation, is suitable over quite a wide range of conditions. The fact that the exponent 1·36 in (22) is found to be almost independent of the gap width suggests that an understanding of the limiting case $d \to 0$ should be relevant to the more general problem.

Landau (1944) has advanced the interesting suggestion that instability may lead to a stable secondary flow, which after a certain increase in velocity would become unstable in turn and be replaced by a still more complex flow. This would continue until eventually the flow is sufficiently disordered as to be considered turbulent. The torque measurements do not appear to show any significant departure from (22) until $T \geqslant 100\,T_c$ and then the points leave the empirical curve fairly slowly. Nothing appears to be as clearly marked as the first instability (cf. Donnelly 1958, Figs. 4, 7). On the other hand, the torques are averaged over considerable fluctuations in the range above Ω_c, which makes it difficult to measure with the precision which one can obtain below Ω_c. Torque measurements alone are not likely to be sufficient to explore the transition to turbulence. Schultz-Grunow and Hein have compared their finite amplitude experiments with Wendt's torque data. They show that at certain Reynolds numbers the regular cells which form after instability begins are perturbed by tangential waves and eventually change their spacing. These details can be correlated with details in the torque measurements.

We have explored the range above Ω_c in figure 8 (which is quite regular) with a visual technique similar to that of Schultz-Grunow and Hein, as well as with ink traces. The wide gap apparatus of Donnelly & Fultz (1960) was used. Here we find that the cell spacing continues to be regular up to speeds corresponding to the limit of measurements in figure 8. The motions in the cells, however, show features which would have to be reported in more detail than can be done at present (see Donnelly & Fultz 1960).

6. The variation of torque with gap width

The variation of G with gap width is, of course, completely specified for laminar flow by (1). The dependence of G upon gap width just above Ω_c is not immediately clear, but for higher values of Ω_1 appears to show significant regularities. For purposes of analysis we might assume, following (16), that the form for G is

$$G/\rho h \Omega_1^2 R_1^4 \propto R^{-l}(d/R_1)^m. \tag{23}$$

From (17), (21), (22) and (23) we see that $l = 2 - n \doteqdot 0{\cdot}64$.

If we plot $\log(G/\rho h\Omega_1^2 R_1^4)$ as a function of $\log R$ and if the proportionality constant in (23) is independent of geometry, then curves corresponding to different values of d/R_1 will be equally spaced for all values of R (provided we avoid the region near Ω_c). A particularly striking example of this is given by the measurements

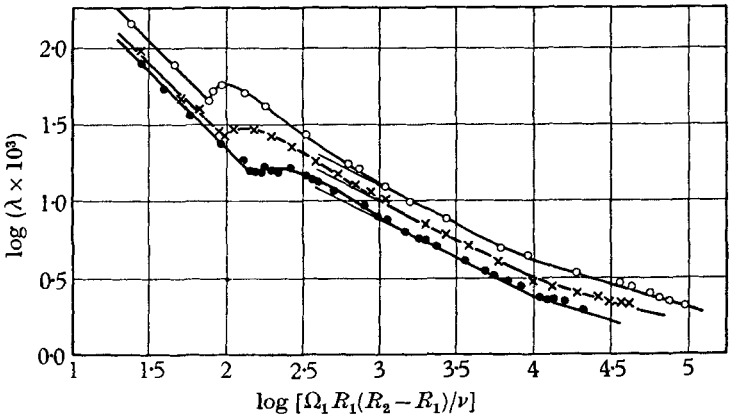

FIGURE 10. Reproduction of Abb. 13 of Wendt's paper. The solid lines represent the empirical equations (24) given by Wendt (1933). R_2-R_1: ○, 4·70 cm; ×, 2·20 cm; ●, 0·95 cm.

of Wendt shown in figure 10. Wendt has drawn the straight lines according to the empirical formulae

$$\lambda = 0{\cdot}46\left[\frac{(R_2-R_1)R_2}{R_1^2}\right]^{\frac{1}{4}} R^{-0{\cdot}5} \quad (4\times10^2 < R < 10^4), \tag{24a}$$

$$\lambda = 0{\cdot}073\left[\frac{(R_2-R_1)R_2}{R_1^2}\right]^{\frac{1}{4}} R^{-0{\cdot}3} \quad (R > 10^4). \tag{24b}$$

We see that (24*a*) implies a variation of torque with Reynolds number similar to what we have proposed in § 4 for $\Omega \gg \Omega_c$ (i.e. $n = 1{\cdot}5$ in (21)). From an inspection of figures 2–5 it can be seen that $n = 1{\cdot}5$ ($l = 0{\cdot}5$) is probably a better choice in this high speed region than $n = 1{\cdot}36$ which was chosen for the best fit closer to Ω_c. This, of course, is the sort of limitation one expects in a purely empirical analysis. It is also interesting to notice from figure 10 and equation 24*b* that the curves are still approximately equally spaced after the bend in the torque curves at $R = 10^4$.

The value of m can be determined from measurements on figure 10 by measuring the distance between any two curves, denoted a and b.

$$\log\lambda_b - \log\lambda_a = m\log[(d/R_1)_b/(d/R_1)_a]. \tag{25}$$

We can also follow Wendt's suggestion given in (24) that dR_2/R_1^2 is the correct parameter and define m' from

$$\log\lambda_b - \log\lambda_a = m'\log[(dR_2/R_1^2)_b/(dR_2/R_1^2)]. \tag{26}$$

Results of such calculations are shown in table 4. They show that for $\log R > 3{\cdot}0$ the values of m (or m') are roughly constant, and that m is not very sensitive to a change in comparison between sets of curves with a ratio $(d/R_1)_b/(d/R_1)_a$ of 2·55 to 6·80.

The measurements by Donnelly can be used again for a comparison between large and small gap widths: $(d/R_1)_b/(d/R_1)_a = 18{\cdot}8$. Beginning with the data in tables 1 and 2 we have computed the quantity

$$\Lambda = G/\rho\Omega_1^2 R_1^4 = G(d/\nu)^2/\rho R^2 R_1^2, \tag{27}$$

and found the ratio Λ_b/Λ_a as a function of R. Here Λ_b refers to the narrow gap measurements. Values of m and m' are compiled as before and the results are given in table 5. We see that over the range $400 < R < 1200$ a constant value of $m = 0{\cdot}35$ will describe the data. Furthermore, the value of m is not much changed from values in table 4 for smaller gap-width ratios.

(*a*) Comparison of Wendt's curves in figure 10 for gap widths 0·95 and 2·20 cm

log R	log λ_b/λ_a	m	m'
2·5	0·148	0·36	0·33
3·0	0·123	0·30	0·28
3·5	0·121	0·30	0·27
4·0	0·121	0·30	0·27
4·5	0·121	0·30	0·27

(*b*) Comparison of curves in figure 10 for gap widths 0·95 and 4·70 cm

2·5	0·277	0·33	0·30
3·0	0·212	0·26	0·23
3·5	0·220	0·26	0·24
4·0	0·224	0·27	0·24
4·5	0·227	0·27	0·24

TABLE 4

R	Λ_b/Λ_a	m	m'
200	0·271	0·45	0·36
300	0·311	0·40	0·33
400	0·342	0·37	0·30
500	0·355	0·35	0·29
600	0·343	0·36	0·30
700	0·348	0·36	0·29
800	0·353	0·35	0·29
900	0·353	0·35	0·29
1000	0·357	0·37	0·29
1100	0·358	0·35	0·29
1200	0·357	0·35	0·29

TABLE 5. Comparison of Donnelly's measurements for gap widths 0·1 and 1·0 cm

Taylor's measurements are not as conclusive as the other experiments on this particular point. His curves extend to higher Reynolds numbers and are not always parallel. This can be seen in Fig. 10 of Taylor's paper (1936) on which are plotted $G/(\rho\Omega_1^2 R_1^2 R_2^2)$ *vs* R for a series of 8 different inner cylinders. We have calculated values of Λ as in (27) for several of Taylor's curves excluding the highest speeds. The results for m are summarized in table 6. We see that, up to log $R = 4$, the values of m are fairly constant and do not vary very much with change in gap width. An exception is seen in table 6*c*, where two wide gap cases

are compared and m is considerably lower. However, the curves lie so close that the error in this determination could be rather large.

We conclude that (23) will represent approximately the data in the speed range considered. The value of m is about $0{\cdot}32 \pm 0{\cdot}05$ and is not very sensitive to the ratio of gap widths being compared. Wendt's suggestion that $(dR_2/R_1^2)^{m'}$ should replace $(d/R_1)^m$ in (23) does not seem to lead to much improvement, as seen in tables 4–6. The results of this section are consistent with the relation (18) proposed by Batchelor, in which the value of m is 0·25.

(*a*) Comparison of Taylor's measurements for gap widths 0·16 and 0·46 cm

log R	log Λ_b/Λ_a	m	m'
3·1	0·166	0·34	0·31
3·3	0·173	0·35	0·33
3·5	0·173	0·35	0·33
3·7	0·180	0·37	0·34
3·8	0·184	0·37	0·35
	(*b*) Comparison for gap widths 0·16 and 0·85 cm		
3·3	0·262	0·32	0·29
3·5	0·255	0·31	0·28
3·7	0·266	0·33	0·30
3·8	0·272	0·34	0·30
	(*c*) Comparison for gap widths 0·60 and 0·85 cm		
3·3	0·048	0·26	0·22
3·5	0·038	0·21	0·18
3·8	0·041	0·22	0·19
4·0	0·042	0·23	0·19

TABLE 6

7. Conclusions

We have analysed the results of a number of measurements of the torque transmitted to an outer cylinder as a function of the angular velocity of the inner cylinder. The results show that the analysis of Stuart (1958) gives the correct variation of torque for a short range above the critical speed. With one exception (figure 5) we find that the functional form

$$G = a\Omega_1^{-1} + b\Omega_1^n \quad (\tfrac{4}{3} < n < \tfrac{3}{2})$$

describes the measurements over a range of about ten times the critical velocity. Details of the range of validity of this equation are given in table 3. The exponent n is not sensitive to the width of the gap between cylinders. A good compromise value appears to be $n = 1{\cdot}36$ for the range indicated in table 3 and $n = 1{\cdot}5$ at higher speeds. When measurements are pushed far enough the empirical relation breaks down.

For speeds well beyond critical it is possible also to describe the variation of torque with gap by

$$G/(\rho h \Omega_1^2 R_1^4) \propto R^{-l}(d/R_1)^m,$$

where $l = 2 - n \doteqdot 0{\cdot}5$ and $m \doteqdot 0{\cdot}31$. This is in fair agreement with the formula (18) obtained by Batchelor (see the appendix).

The authors are indebted to Dr J. T. Stuart for supplying the numerical result in (12) and for discussions of his theory. We owe to Dr G. K. Batchelor the suggestion that we investigate the variation of torque with gap width at high speeds. Dr G. Veronis has assisted us with discussions and suggestions on the manuscript.

The research described here has been supported, in part, by a grant (NSF G-3489) from the National Science Foundation. One of us (R. J. D.) is indebted to the Alfred P. Sloan Foundation for a Research Fellowship.

Appendix

A theoretical model of the flow at speeds far above the critical

By G. K. Batchelor (University of Cambridge)

After Dr Donnelly and Miss Simon had prepared their paper for publication, I noticed that the empirical relation between torque G and angular velocity Ω_1 at speeds well above the critical (viz. that $G \propto \Omega_1^n$ where n is about 1·5) is in accord with a prediction based on a simple theoretical model of the flow. This theoretical model also gives a prediction of the dependence of G on the size of the gap between the cylinders at speeds well above the critical; and it seems from further analysis of the available data by Donnelly and Simon, now incorporated in the paper, that the theoretical and observed relationships are again in fair agreement. It therefore seems worthwhile to record here the basis of the theoretical results.

It is supposed, first, that the flow between the two cylinders is steady, even though the angular velocity of the inner cylinder is far above the critical value. This steady flow will presumably have a cellular form, with the same axial wavelength as at speeds just above the critical although certainly not with the same velocity distribution, and the streamlines will lie on closed surfaces of revolution. When the angular velocity Ω_1 is large enough, the Reynolds number of the motion in an axial plane will be large compared with unity, and the whole flow will consist of regions in which viscous forces are negligible and thin layers in which viscous forces are significant. The distribution of vorticity in the inviscid core of flow systems of this kind has been investigated (Batchelor 1956), but no use of the detailed form of the velocity or vorticity distributions will be made here. For the present purpose (which is to predict the functional dependence of torque on angular velocity Ω_1 and gap d, without bothering about the numerical value of constants of proportionality) it is sufficient to assume a flow in the axial plane of the kind sketched in figure 11. In this figure δ represents the general magnitude of the thickness of the boundary layer round the outside of the inviscid core of one cell, and we shall write v for the velocity (in the axial plane) at the outer edge of this inviscid core.

We now estimate δ and v in terms of d and Ω_1. One relation is obtained by assuming the usual parabolic growth of a boundary layer with distance. The boundary layer under discussion is closed, and its thickness increases over part of its length and decreases over the remainder (the decrease occurring because the centrifugal force accelerates the fluid in the boundary layer over the horizontal parts of its length), but the general magnitude of the thickness will presumably be

the same as if the layer had increased in thickness over a path of length of order d under the action of an external stream velocity of order v. Thus we have

$$\frac{\delta}{d} \sim \left(\frac{dv}{\nu}\right)^{-\frac{1}{2}}. \tag{A 1}$$

A second relation follows from the balance in the boundary layer between the driving centrifugal force and the retarding viscous force. Fluid very close to the inner cylinder is acted on by centrifugal force $\Omega_1^2 R_1$, whereas fluid close to the stationary outer cylinder is subject to no centrifugal force. The general magnitude

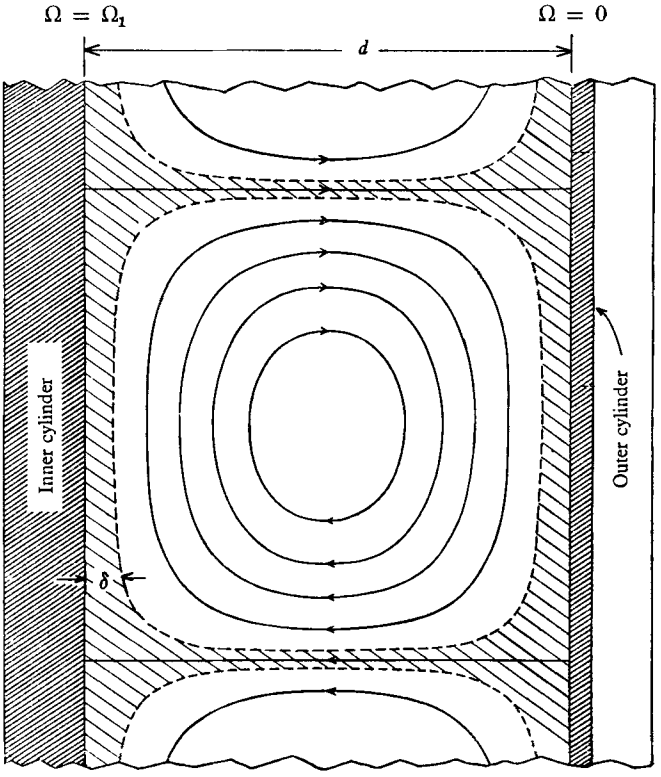

FIGURE 11. Sketch of the flow (in an axial plane) assumed in the theoretical argument. The lightly shaded area represents the boundary layer region in which viscous forces are significant.

of the centrifugal force acting on fluid throughout the boundary layer is thus $\Omega_1^2 R_1$, whereas that of the viscous force per unit mass, in the direction of flow in the axial plane, is $\nu v/\delta^2$. Hence

$$\Omega_1^2 R_1 \sim \nu v/\delta^2. \tag{A 2}$$

The relations (A 1) and (A 2) together give

$$v \sim \Omega_1 (dR_1)^{\frac{1}{2}}, \quad \delta \sim d^{\frac{1}{4}} \nu^{\frac{1}{2}} / \Omega_1^{\frac{1}{2}} R_1^{\frac{1}{4}}. \tag{A 3}$$

The corresponding Reynolds number of the axial boundary-layer flow is thus

$$\frac{v\delta}{\nu} \sim \left(\frac{\Omega_1 R_1 d}{\nu}\right)^{\frac{1}{2}} \left(\frac{d}{R_1}\right)^{\frac{1}{4}},$$

and this is the number which must be large compared with unity for the analysis to be applicable. This requirement was certainly satisfied in some of the experiments described in the paper; for instance, in Donnelly's (1958) experiments with the smaller of his two inner cylinders, $d/R_1 = 1{\cdot}0$ and the Reynolds number $\Omega_1 R_1 d/\nu$ ranged up to about 2000.

The torque G acting on a length h of the inner cylinder can now be determined from the fact that the azimuthal velocity of the fluid drops from $\Omega_1 R_1$ at the cylinder to some value representative of the core conditions in a distance δ. The distribution of angular velocity Ω in the inviscid core is such (Batchelor 1956) as to make the circulation about the inner cylinder uniform (i.e. $\Omega \propto r^{-2}$) and equal to some value intermediate between $2\pi\Omega_1 R_1^2$ and zero, so that Ω must change by an appreciable fraction of its value across the boundary layer. Hence

$$\begin{aligned} G &\sim hR_1^2 \times \text{viscous stress at cylinder} \\ &\sim hR_1^2\left(\frac{\mu\Omega_1 R_1}{\delta}\right) \\ &\sim h\rho\Omega_1^2 R_1^4\left(\frac{\nu}{\Omega_1 R_1 d}\right)^{\frac{1}{2}}\left(\frac{d}{R_1}\right)^{\frac{1}{4}}, \end{aligned} \tag{A 4}$$

which is the relation (18) quoted in the paper. It is to be noted that this relation is an asymptotic one, holding more closely as the Reynolds number of the flow increases. It seems reasonable to infer, from the agreement between (A 4) and some of the observations discussed in the paper, that a flow of the type sketched in figure 11 does in fact occur under the conditions of these same observations.

REFERENCES

Batchelor, G. K. 1956 *J. Fluid Mech.* **1**, 177.

Chandrasekhar, S. 1954 *Mathematica*, **1**, 5.

Chandrasekhar, S. 1958 *Proc. Roy. Soc.* A, **246**, 301.

Donnelly, R. J. 1958 *Proc. Roy. Soc.* A, **246**, 312.

Donnelly, R. J. & Fultz, D. 1960 *Proc. Roy. Soc.* A (to be published).

Landau, L. 1944 *C.R. Acad. Sci. U.S.S.R.* **44**, 311.

Schultz-Grunow, F. & Hein, H. 1956 *Z. Flugwiss.* **4**, p. 28.

Stuart, J. T. 1958 *J. Fluid Mech.* **4**, 1.

Taylor, G. I. 1923 *Phil. Trans.* A, **223**, 289.

Taylor, G. I. 1936 *Proc. Roy. Soc.* A, **157**, 546.

Wendt, F. 1933 *Ingen.-Arch.* **4**, 577.